frontiers | Frontiers in Earth Science

TYPE Original Research
PUBLISHED 27 December 2023
DOI 10.3389/feart.2023.1293648

OPEN ACCESS

EDITED BY
Wei Shi,
Chengdu University of Technology, China

REVIEWED BY
Xinli Zhao,
Changzhou University, China
Jizhen Zhang,
Yangtze University, China
Debin Xia,
Chinese Academy of Sciences (CAS), China

*CORRESPONDENCE
Ying Guo,
guoying@lyu.edu.cn
Jian Li,
lijian69@petrochina.com.cn

RECEIVED 13 September 2023
ACCEPTED 31 October 2023
PUBLISHED 27 December 2023

CITATION
Shi J, Guo Y, Li J, Du G, Jing X, Liu G, Huang J, Fang C and Zhang T (2023), Geochemical characteristics and genesis of the Ordovician sub-salt natural gas in the Ordos Basin, China.
Front. Earth Sci. 11:1293648.
doi: 10.3389/feart.2023.1293648

Geochemical characteristics and genesis of the Ordovician sub-salt natural gas in the Ordos Basin, China

Jianglong Shi[1], Ying Guo[2]*, Jian Li[3]*, Guanghong Du[4], Xianghui Jing[4], Gang Liu[4], Junping Huang[1], Chenchen Fang[3] and Tingting Zhang[5]

[1]PetroChina Research Institute of Petroleum Exploration and Development Northwest Branch, Lanzhou, China, [2]Institute of Geology and Paleontology, Linyi University, Linyi, China, [3]PetroChina Research Institute of Petroleum Exploration and Development, Beijing, China, [4]Exploration and Development Institute of PetroChina Changqing Oilfield Company, Xi'an, China, [5]Gansu Non-Ferrous Metal Geological Exploration Bureau, Lanzhou, China

A significant amount of natural gas resources has been discovered in the Ordovician reservoirs under a thick layer of gypsum-salt strata as a result of ongoing research into deep natural gas in China's Ordos Basin, however, the genetic type and source of the Ordovician sub-salt natural gas remain contentious. These limits understanding how the geochemical properties of the natural gas in Ordos Basin have evolved and how to best guide future exploration and development. Based on the components, carbon and hydrogen isotopic ratios of natural gas from the latest exploration wells, combined with the geological background, this study systematically analyzed the genetic types and sources of sub-salt natural gas of the central and eastern Ordos Basin. The results show that the Ordovician natural gas is mainly composed of hydrocarbon gases with low content of heavy hydrocarbons and dryness (C_{CH4}/C_{CH4+}) above 0.95, belonging to typical dry gas. Non-hydrocarbon gases mainly include N_2 and CO_2, and some natural gas samples contained H_2S. The Ordovician sub-salt natural gas is primarily a self-generating and self-preserving oil-cracking gas with relatively high maturity (Ro ranging from 1.5% to 2.1%) mixed with coal-derived gas generated from upper-Paleozoic coal with relatively low maturity (Ro ranging from 1.1% to 1.5%). Due to the dual-source hydrocarbon supply, the Ordovician sub-salt reservoirs provide favorable gas accumulation conditions and development prospects. This study offers a reasonable explanation for the anomalous geochemical characteristics of the Ordovician sub-salt reservoirs in the Ordos Basin, and also may serve as a guide for future exploration of natural gas in the carbonate gypsum-salt sedimentary system in other basins.

KEYWORDS

genesis, natural gas, Ordovician, geochemical characteristic, Ordos Basin

Abbreviations: $\delta^{13}C$, carbon isotopic composition of alkane; C_{CH4}/C_{CH4+}, dryness coefficient; GC, gas chromatograph; O_1m_1, the 1st member of Majiagou Formation; $O_1m_5{}^1$, the 1st sub-section of the 5th member of Majiagou Formation; Ro, vitrinite reflectance; TCD, thermal conductivity detector; TSR, thermochemical sulfate reduction.

1 Introduction

China is endowed with abundant natural gas resources, and its onshore natural gas is mainly distributed in the Ordos Basin, Sichuan Basin, and Tarim Basin (Fu et al., 2019; Li et al., 2019). By 2020, the annual hydrocarbon production of the whole basin reached 7,900 × 10^4 t oil equivalent, making the Ordos Basin the largest producer among all petroliferous basins in China (Li et al., 2018; Ren et al., 2021a). At present, the main natural gas reservoirs of the Ordos Basin are concentrated in the upper Paleozoic and Mesozoic (Jia et al., 2014; Li, 2021a). Exploration for hydrocarbons in the medium-shallow layers of the Ordos Basin is now facing growing difficulties in discovering major oil and gas accumulation (Zou et al., 2023). Therefore, it is of great significance to explore deep and ultra-deep mature oil and gas for stabilizing production and finding new domains (Li et al., 2019; Zhao et al., 2020; Dai et al., 2021).

The exploration of natural gas in the lower Paleozoic of the Ordos Basin has been initiated long ago. In 1987, Well Sc-1 made the first breakthrough in the weathering crust reservoir at the top of the Ordovician in the central paleo-uplift and led to the discovery of the Jingbian gas field (He et al., 2022). This solidly demonstrated the favorable conditions of the lower Paleozoic for hydrocarbon accumulation as well as its high exploration potential. Recently, Wells Mt-1 and T-38 delivered high-rate industrial gas streams from layers below the thick gypsum salt formation, which further expanded the potential field of natural gas exploration in the Ordovician sub-salt and deep layers.

Numerous studies have been carried out on the genesis of the lower Paleozoic natural gas in the Ordos Basin. Some claim that the thick gypsum salt rock in the middle Ordovician has good sealing performance, and the sub-salt natural gas is oil-type gas generated by the low organic matter marine source rock in the lower Ordovician, which belongs to self-generating and self-storing natural gas (Li et al., 2017; Kong et al., 2019; Zou et al., 2023). Another view is that the sub-salt low organic matter abundance marine source rock has a limited hydrocarbon generation capacity and the natural gas is coal derived gas generated from Carboniferous-Permian coal bearing series and transported via lateral migration (Dai et al., 2014; Ren et al., 2021b; Bao et al., 2023). There will be more doubt about the distribution and development prospects natural gas when its genesis and type remain unclear. The Ordovician sub-salt of the Ordos Basin's natural gas development will be severely limited as a result. Thus, the genetic type, source, and accumulation mode of Ordovician sub-salt natural gas are further analyzed in this study based on the natural gas composition, carbon isotope, and hydrogen isotope of the most recent exploration wells, along with the geological features. This will provide scientific proof for the exploration of Ordovician natural gas in the Ordos Basin.

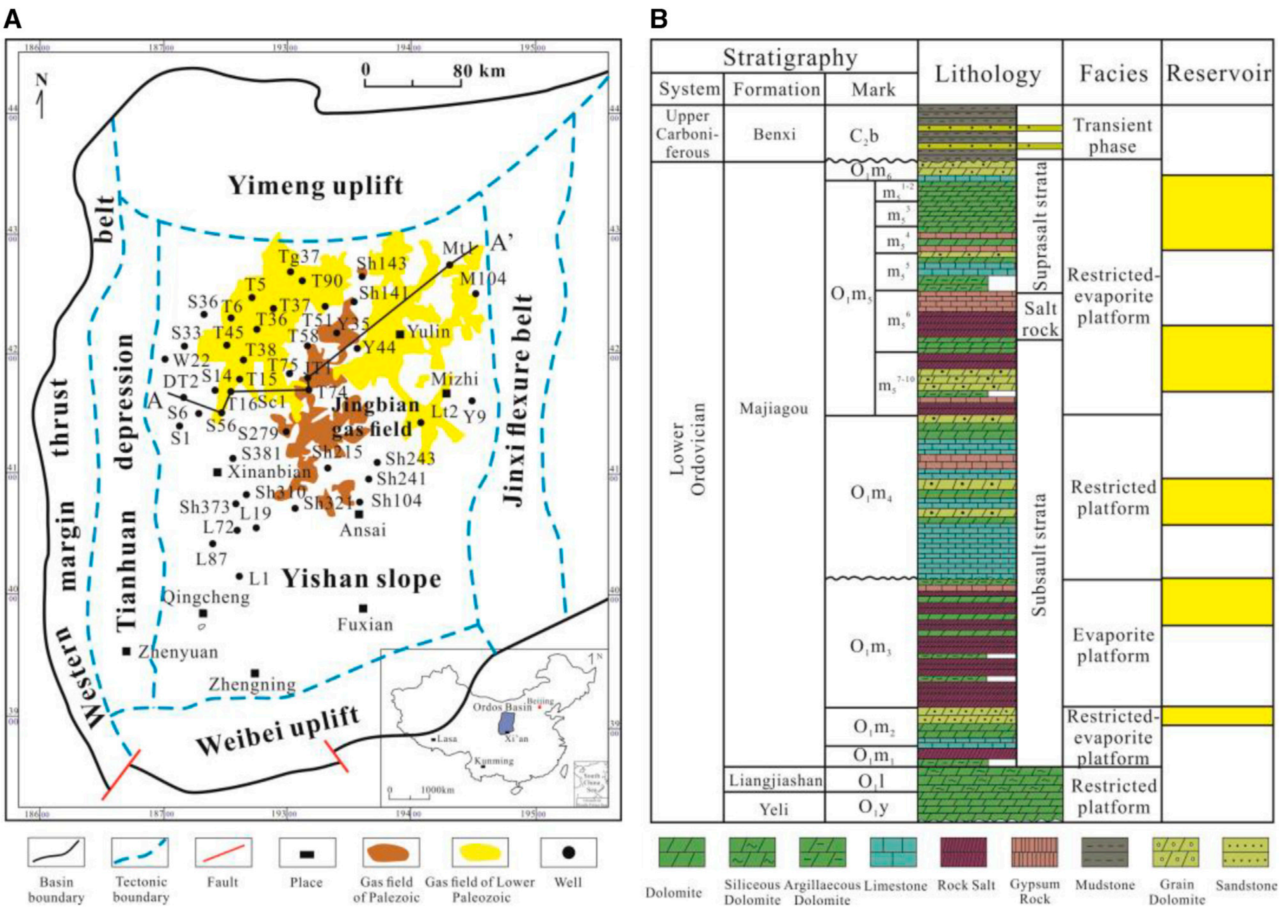

FIGURE 1
Structural units **(A)** and lower Ordovician stratigraphic column **(B)** of the Ordos Basin (Niu et al., 2019; Wu et al., 2021, Modified).

2 Geological background

The Ordos Basin is located in central China which tectonically belongs to the western edge of the North China Block (Du et al., 2019; Fu et al., 2021a; Figure 1A). It is the second largest continental basin in China covering an area of approximately 25 × 10^4 km^2 (Feng et al., 2016). The Ordos Basin can be divided into six structural units, including the Western margin thrust fold belt, Tianhuan depression, Yimeng uplift, Yishan slope, Weibei uplift, and Jinxi flexure belt (Fu et al., 2006; Li et al., 2021b). Among them, Yishan slope is the most important tectonic unit for oil and gas accumulation. The sedimentary evolution of the lower Paleozoic carbonate rocks in the Ordos Basin is mainly controlled by a paleo-structural framework. From the late Cambrian to the early Ordovician, the Wushenqi-Jingbian area was uplifted by the Yimeng paleo-uplift (Liu et al., 2021). Its periphery gradually dips toward the sea and the lower Ordovician Yeli-Liangjiashan Formation is deposited around the platform with a predominant lithology of dolomite and siliceous dolomite. During this period, the subduction of the Qinling-Qilianshan oceanic crust gradually uplifted and formed the L-shaped central paleo-uplift, which controlled the Mizhi-Zizhou sub-sag, the Yimeng paleo-land and Luliang low uplift (Fu et al., 2021b; Ren et al., 2021b). The Ordovician in the central and eastern Ordos Basin is developed in the lower and middle series, and the upper Ordovician was eroded by the uplift of the strata.

The lower Ordovician and middle Ordovician successively developed Yeli Formation, Liangjiashan Formation and Majiagou Formation from bottom to top (Figure 1B). According to its sedimentary evolution characteristics, the Majiagou Formation is divided into 6 members. The 1st (O_1m_1), the 3rd (O_1m_3) and the 5th (O_1m_5) member of Majiagou Formation deposited at stage of regression period, mainly developed argillaceous dolomite, mudstone and gypsum-salt rock. O_1m_5 can be divided into 10 sub-sections ($O_1m_5^{1-10}$) in terms of lithology. The 2nd (O_1m_2), the 4th (O_1m_4) and the 6th (O_1m_6) member of Majiagou Formation deposited at stage of transgression period, and the lithology is mainly micrite limestone (Wu et al., 2021; Figure 1B). Due to the large sedimentary thickness and wide distribution range of the gypsum-salt rock in the 6th sub-section of the 5th member of Majiagou Formation ($O_1m_5^6$), the Ordovician Majiagou Formation is divided into suprasalt strata ($O_1m_5^1$-$O_1m_5^5$) and sub-salt strata ($O_1m_5^6$-O_1m_1). And this set of gypsum-salt rock is also a good regional cap rock in the central and eastern part of the basin. Ordovician Majiagou Formation is a marine source rock with low organic matter abundance (Liu et al., 2016), which cannot meet the standard of high-quality source rock in the traditional hydrocarbon source evaluation system. However, this layer has obtained high-rate industrial gas streams in wells Mt-1 and T-38 at present, so there are doubts about the natural gas source of the Lower Paleozoic Ordovica in the Ordos Basin.

3 Sampling and analytical methods

3.1 Sampling

Seventeen gas samples were collected from producing wells drilled into the Ordovician Majiagou Formation of the Ordos Basin. Among them, 11 samples were acquired in the $O_1m_5^{6-10}$, 5 samples in the O_1m_4, and 1 sample was taken from the O_1m_3. Natural gas samples were obtained using high pressure steel cylinders with valves at both ends. The cylinders were flushed with natural gas at the high-pressure wellhead for 10–15 min to remove air prior to sampling. The composition of the gas samples, as well as their carbon and hydrogen isotopic ratios were measured within 15 days after sampling. In order to compare with Ordovician natural gas, this study collected natural gas geochemical data of 17 wells from upper Paleozoic in the Changqing Oilfield.

3.2 Analytical methods

The collected gas samples were tested at the PetroChina Research Institute of Petroleum Exploration and Development Langfang Branch, China. Gas compositions were analyzed via an Agilent 6890 N Gas Chromatograph (GC) installed with a thermal conductivity detector (TCD), using helium (He) as the carrier gas. Individual gases were segregated by the PLOT Q capillary column equipped with the size of 30 m × 0.53 mm × 25 μm. The inlet temperature was set at 150°C and the TCD temperature was 200°C. The programmed GC oven had an initial temperature of 40°C which was held for 7.5 min, then raised to 90°C at a rate of 15°C/min, and finally raised to 180°C at a rate of 6°C/min.

The carbon isotopic compositions of gases were determined on a Delta S isotopic mass spectrometer (Thermo Fisher Scientific) equipped with an Agilent 6890 N GC. Individual hydrocarbon gas compound (C_1-C_5) was separated using a HP-PLOT Q capillary column with the size of 30 m × 0.32 mm × 20 μm. The GC oven was initially held at 30°C for 5 min, followed by raising to 80°C at a rate of 8°C/min and then to 170°C at 5°C/min, and finally to 270°C at 6°C/min. The oxidation oven temperature for converting individual hydrocarbon compounds to CO_2 was 950°C.

The hydrogen isotopic compositions of gases were measured by a MAT253 isotopic mass spectrometer (Thermo Fisher Scientific) equipped with a Trace GC Ultra™ using the gas chromatography pyrolysis interface and the removing water device. Helium was used as the carrier gas equipped with a 30 m × 0.32 mm × 20 μm HP-PLOT Q column was used with flow rate of 1.4 mL/min. The inlet temperature was set at 180°C. A split injection mode (split ratio 1:7) was used for the methane hydrogen isotope measurement and a splitless injection mode for the ethane and propane hydrogen isotopes. The initial temperature was 40°C and held for 5 min, then heated from 40°C to 80°C at 5°C/min, from 80°C to 140°C at 10°C/min and from 140°C to 260°C at 30°C/min, respectively. The temperature of the pyrolysis oven was 1,450°C, and gaseous hydrocarbon components were transformed into C and H_2. The H_2 went into mass spectrometer to be measured. The δD was calculated relative to V-SMOW. The reproducibility and precision of hydrogen isotope value are less than ±3‰.

4 Results

4.1 Natural gas composition

The hydrocarbon composition of the Ordovician natural gas in the Ordos Basin was predominately CH_4 with a large variation

TABLE 1 Composition and isotope of natural gas in the Ordos Basin.

Well	Formation	Natural gas components (%)							Dry cofficient (C_{CH4}/ C_{CH4+})	$\delta^{13}C$ (‰), V-PDB				δD (‰)		
		CH_4	C_2H_6	C_3H_8	C_{4+}	N_2	CO_2	H_2S		CH_4	C_2H_6	C_3H_8	n-C_4	CH_4	C_2H_6	C_3H_8
Sh-373	O_1m^6	92.45	0.24	0.02	0.00	2.28	5.00		0.99	−34.35	−33.65	−26.84				
S-381	$O_1m_5^6$	92.43	0.14	0.01	0.00	3.98	3.44		0.99	−35.95	−34.51					
T-45	$O_1m_5^6$	95.03	0.73	0.05	0.99	2.60	1.51		0.98	−39.10	−35.60	−26.70	−24.70			
L-72	$O_1m_5^6$	87.20	0.18	0.02	0.00	6.14	6.46		0.99	−33.06	−34.33	−31.11				
L-87	$O_1m_5^7$	78.48	0.29	0.03	0.00	11.08	10.11		0.99	−33.46	−35.04	−32.82				
T-74	$O_1m_5^7$	88.62	0.73	0.12	0.99	8.31	0.82	1.27	0.98	−39.50	−29.90	−21.70	−20.20			
T-75	$O_1m_5^7$	85.04	1.59	0.30	0.98	2.30		9.02	0.97	−32.40	−22.60	−22.40	−21.80			
T-58	$O_1m_5^7$	82.96	0.05	0.03	1.00	1.85	2.41	12.73	0.99	−33.40						
Tg-37	$O_1m_5^{10}$	88.05	0.08	0.01	0.01	5.67	6.17		0.99	−38.20	−30.71					
T-38	$O_1m_5^{10}$	89.41	0.19	0.19	1.00	0.17	0.14	9.90	0.98	−36.90	−25.60					
JT-1	$O_1m_5^{10}$	85.68	0.01	0.36	1.00	0.28	0.26	13.31	0.98	−36.62	−23.00			−153	−120	−101
T-36	O_1m_4	92.43	0.78	0.14	0.08	2.72	3.81		0.99	−34.54	−24.65	−24.49				
Tg-51	O_1m_4	92.10	1.20	0.40		1.95	0.21	5.01	0.98	−42.30	−25.90	−23.14		−158	−112	−102
M-104	O_1m_4	97.71	1.03	0.29		0.22	0.27		0.99	−42.26	−25.38	−20.53				
Mt-1	O_1m_4	93.27	3.08	0.97	0.81	0.86	0.52	3.49	0.95	−44.80	−27.70	−25.10	−23.80	−171	−125	−115
T-37	O_1m_4	88.05	0.08	0.01		5.67	6.17		0.99	−38.20	−30.71					
T-90	O_1m_3	94.86	1.13	0.11		0.43	0.20	3.30	0.99	−41.50	−30.50	−26.30				
S-1	P_1s	91.57	4.52	0.89		0.71	0.78		0.94	−34.37	−22.13	−21.77				
S-6	P_1x	88.81	5.83	1.26		0.80	2.64		0.93	−33.54	−24.02	−24.72				
S-14	P_1x	96.37	1.66	0.40		0.70	1.25		0.98	−32.54	−23.17	−23.77				
S-33	P_1x	91.69	4.26	0.91		1.43	0.87		0.95	−32.31	−25.23	−23.79				
S-36	P_1x	89.49	5.41	1.16		0.93	0.76		0.93	−33.40	−24.70	−24.40				
T-5	P_1x	91.75	5.11	0.92		1.05	0.77		0.94	−33.05	−23.57	−23.72				
T-6	P_1x	93.40	2.76	0.36		2.27	0.57		0.97	−29.00	−25.00	−27.00				
Sh-141	P_1s	94.12	3.40	0.50		0.61	1.14		0.96	−33.70	−26.30	−24.30				
Sh-143	P_1s	93.47	3.90	0.63		0.35	1.17		0.95	−33.57	−25.98	−24.42				
Y-35	P_1s	95.32	2.67	0.34		0.03	1.45		0.97	−31.55	−24.87	−23.69				
Y-44	P_1s	95.65	2.65	0.32		0.69	0.57		0.97	−32.80	−25.50	−23.80				
Sh-215	P_1x	93.60	3.79	0.55		0.46	0.76		0.96	−32.90	−26.00	−24.00				
Sh-241	P_1x	92.70	3.99	0.68		1.73	0.49		0.95	−32.60	−24.10	−24.20				
Sh-243	P_1x	90.85	5.46	1.03		1.55	0.54		0.93	−35.00	−24.00	−23.60				
W-22	P_1x	92.97	4.27	0.76		0.87	0.74		0.95	−32.60	−23.70	−24.20				
Y-19	P_1x	92.79	3.90	0.64		1.77	0.50		0.95	−34.50	−23.70	−24.70				
Y-24	P_1x	92.77	4.21	0.63		1.43	0.64		0.95	−32.20	−23.50	−24.90				

content of heavy hydrocarbons (Table 1). The average content of CH_4 and heavy hydrocarbon of natural gas from O_1m_3-O_1m_4 is 91.52% and 1.32% respectively, with dryness coefficient (C_{CH4}/ C_{CH4+}) above 0.95 which is typical dry gas. The average content of CH_4 and heavy hydrocarbon of natural gas from $O_1m_5^{6-10}$ is 88.43% and 1.25%, respectively, with dryness coefficient above 0.97 which also represents a typical dry gas (Figure 2). In contrast, the CH_4 content of natural gas from the upper

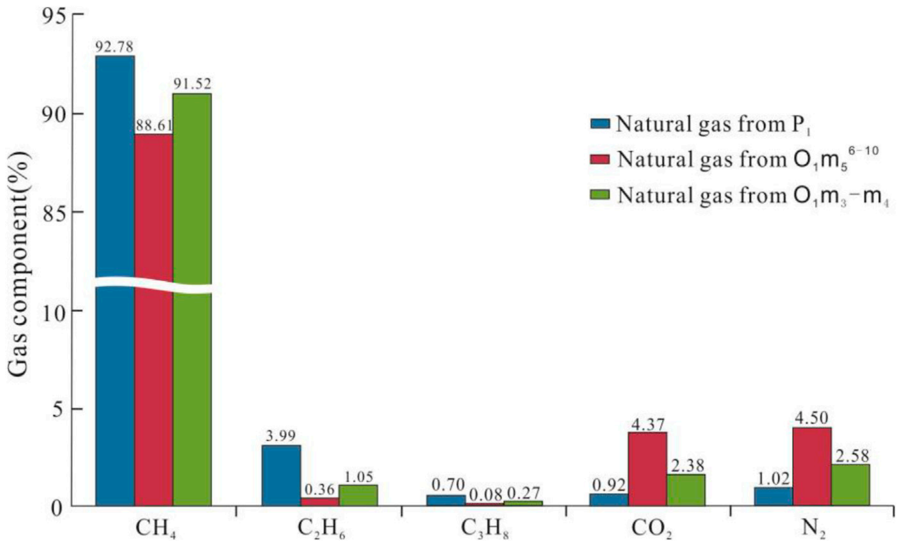

FIGURE 2
Relative proportions of gas components of Ordovician natural gas in the Ordos Basin.

Paleozoic ranged from 88.81% to 96.37% with an average of 92.78%, while the average content of heavy hydrocarbon content was 4.7% with the dryness coefficient ranges from 0.93 to 0.98 (average 0.95) which indicates the predominance of dry gas.

Non-hydrocarbon components of the natural gas mainly include N_2 and CO_2. Some Ordovician natural gas samples contain H_2S ranging from 1.27% to 13.31%. According to the classification standard of H_2S content in natural gas, these samples belong to minor to high H_2S content natural gas (Zhu et al., 2004). The N_2 and CO_2 content in the upper Paleozoic natural gas were relatively low with average content of 1.02% and 0.92%, respectively, while that Ordovician natural gas was considerably higher with average content of 3.96% and 3.82%, respectively. Littke et al. (1995) carried out simulations of the N_2 production of organic matter with different maturities, which showed that the production rate of N_2 increased with thermal maturity. Subsequently, many scholars (Liu et al., 2007; Shen et al., 2019) investigated the genesis of N_2 in the lower Paleozoic natural gas of the Tarim and Sichuan Basins and commonly accepted that high N_2 content is mainly generated from muddy carbonate rocks at high to over mature stage. In general, the content of CH_4 increases with the increasing thermal maturity of source rocks at mature to over mature stages, and so does the dryness. Figure 3 shows that the N_2 content and dryness of the Ordovician natural gas were significantly higher than those of the upper Paleozoic natural gas, which is mainly caused by thermal maturity of the natural gas and its sources material types.

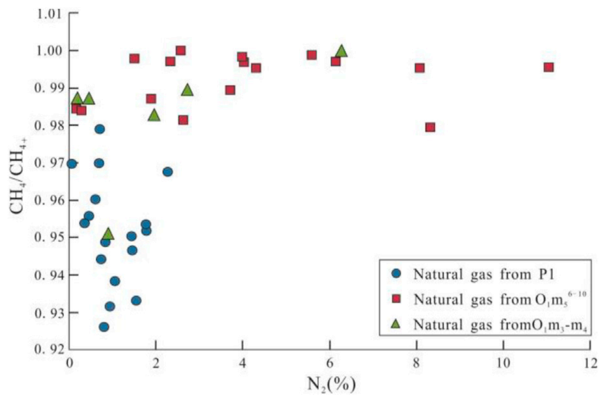

FIGURE 3
Relationship of C_{CH4}/C_{CH4+} and N_2 of natural gas in the Ordos Basin.

4.2 Carbon isotope compositions

The carbon isotopic composition of methane ($\delta^{13}C_1$) of gas samples collected from the upper Paleozoic in the Ordos Basin ranged from −35.0‰ to −29.0‰ with an average of −32.9‰, $\delta^{13}C_2$ ranged from −26.3‰ to −22.1‰ with an average of −24.4‰, and $\delta^{13}C_3$ ranged from −27.0‰ to −21.8‰ with an average of −24.2‰. For the natural gas from $O_1m_5^{6-10}$, $\delta^{13}C_1$ ranges from −44.8‰ to −34.5‰ with an average of −40.18‰, $\delta^{13}C_2$ ranges from −39.4‰ to −22.6‰ with an average of −32.1‰, and $\delta^{13}C_3$ ranges from −32.8‰ to −21.7‰ with an average of −24.2‰. The $\delta^{13}C_1$ of natural gas from O_1m_3 and O_1m_4 ranges from −44.8‰ to −34.5‰ with an average of −40.2‰, $\delta^{13}C_2$ ranges from −31‰ to −24.7‰ with an average of −28.2‰, and $\delta^{13}C_3$ ranges from −26.3‰ to −20.5‰ with an average of −24.2‰. The carbon isotopic composition of alkane gas in the Ordos Basin shows that the natural gas derived from the upper Paleozoic has the heaviest carbon isotopic value, while that from O_1m_3 and O_1m_4 has the lightest carbon isotopic value, and that from $O_1m_5^{6-10}$ is between the above them (Table 1).

5 Discussion

5.1 Genesis of natural gas

The carbon isotope composition of organic natural gas is characterized by the trend $\delta^{13}C_1 < \delta^{13}C_2 < \delta^{13}C_3 < \delta^{13}C_4$, which is referred to positive carbon isotope sequence, while inorganic natural gas features $\delta^{13}C_1 > \delta^{13}C_2 > \delta^{13}C_3 > \delta^{13}C_4$ is referred to the negative carbon isotope sequence (Dai, 1992). The carbon isotope ratio of alkane gas is a widely used and relatively full-fledged indicative parameter of the genesis, maturity, and gas source correlation of natural gas (Boreham and Edwards, 2008; Burruss and Laughrey, 2010). The causes of an inverted carbon isotope ratio distribution for alkane gas are mainly the following: (1) mixed gas of organic and inorganic alkane gases, (2) mixed gas of oil type and coal generated gases, (3) mixed gas of the same source at different stages or the same type with different source rocks, (4) oxidation of one or more components of alkane gas by bacteria and (5) thermal sulfate reduction (Dai et al., 2003; Tilley and Muehlenbachs, 2013). The natural gas in the Ordos Basin predominately features a positive carbon isotope sequence. The natural gas from O_1m_3 and O_1m_4 presented a positive carbon isotope sequence, while those from $O_1m_5^{6-10}$ and the upper Paleozoic featured the partial carbon isotopic reversal, such as samples L-72, L-87, and S-323 with $\delta^{13}C_1 > \delta^{13}C_2 < \delta^{13}C_3$, and Su-1, S-241, and Y-24 with $\delta^{13}C_1 < \delta^{13}C_2 > \delta^{13}C_3$. The hydrogen isotope of CH_4 of natural gas in the Ordos Basin was between −171‰ and −153‰ (Table 1), and carbon isotope of C_2H_6 was between −39.4‰ and −22.1‰, which suggested typical organic gas.

Although carbon isotope fractionation occurs during long distance migration of natural gas (Prinzhofer and Huc, 1995). The thickness and wide distribution of the gypsum salt rock in the $O_1m_5^6$ has excellent sealing ability and the carbonate reservoirs under the gypsum salt rock have low physical properties which belong to tight reservoir (Wu et al., 2021). It is difficult for the gas to migrate and upper Paleozoic coal derived gas to pour into the carbonate reservoirs. Therefore, the carbon isotope reversal of Ordovician sub-salt natural gas was mainly caused by secondary reaction and the mixing of gases generated by different source rocks.

According to the kerogen pyrolysis model, alkane gas of single source shows a linear relationship between the carbon number (1/n) and $\delta^{13}C_n$ (Chung et al., 1988). The changes in the slope of the regression line can be used to identify mixing between different types of gas at different maturation stages or biogas mixing and monitor the effects of methane leakage (Rooney et al., 1995). The upper Paleozoic gas in the Ordos Basin presented similar distribution characteristics and high linearity of $\delta^{13}C_n$ *versus* 1/n (Figure 4A), which indicated that the natural gas was generated by the same source rocks. The carbon isotope of the gas from O_1m_3 and O_1m_4 varied greatly and the linearity between $\delta^{13}C_n$ and 1/n was relatively high, which implied less gas mixing (Figure 4B). As for the gas from $O_1m_5^{6-10}$, the correlation linearity between $\delta^{13}C_n$ and 1/n was low (Figure 4C), suggesting that the natural gas was mixed gas generated by different source rocks or experienced strong secondary action.

Based on experimental simulations, Bernard et al. (1978) proposed to use the $\delta^{13}C_1$ *versus* $C_1/(C_2 + C_3)$ plot to distinguish different types of natural gas generated by kerogen and this plot has been extensively applied to the genesis identification of natural gas in different basins (Whiticar, 1999). The $\delta^{13}C_1$ *versus* $C_1/(C_2 + C_3)$ plate showed that the Ordovician natural gas in the Ordos Basin mainly originated from type-II kerogen with high maturity and mixed with some natural gas derived from type-II and III kerogen. Moreover, the upper Paleozoic natural gas clearly originated from type-III kerogen with relatively low thermal maturity (Figure 5). Based on the isotopic statistics of natural gas from different basins of China, Li et al. (2017) claimed that the ($\delta^{13}C_2$-$\delta^{13}C_1$) *versus* $\delta^{13}C_1$ plot can distinguish oil-type gas from coal derived gas and used this plot to identify different gas geneses. As illustrated in Figure 6, the upper Paleozoic natural gas in the Ordos Basin was a typical coal derived gas, while Ordovician natural gas was mainly oil-type gas and only part of mixed gas with coal derived gas.

According to the genesis and planar distribution of the natural gas in the central and eastern Ordos Basin, it was found that the Ordovician coal derived gas was primarily distributed near the L-shaped central paleo-uplift with $\delta^{13}C_2$ usually greater than −28‰, which was similar to that of the upper Paleozoic natural gas. Meanwhile, the Ordovician natural gas in the mid-eastern Ordos Basin is oil-type gas with $\delta^{13}C_2$ less than −28‰. During the early Ordovician, the oceanic plates to the north and south dove below the North China plate, which led to the continuous uplifting of the crust of the southwestern Ordos block and the central paleo-uplift with its L-shaped planar morphology (Fu et al., 2021b). Subsequently, rapid transgression during the Ordovician deposited the thick carbonate rocks of the Majiagou Formation and widely spread across the basin. During the middle and late Ordovician, owing to the Caledonian movement, the north China continental plate as a whole was uplifted and the Ordos Basin was subjected to weathering, leaching, and denudation for hundreds of millions of years, which resulted in a thick karst weathering crust unconformity near the central paleo-uplift (Shao et al., 2019; Ren et al., 2021b). The deposition was suspended until the Carboniferous, and thick coal bearing formation system in the swamp littoral facies was widely deposited above the unconformity surface of the Majiagou Formation (Yang et al., 2013). The unconformity formed during the Caledonian period was not only the dominant channel for hydrocarbon migration but also a high-quality reservoir. Near the central paleo-uplift, the coal derived gas was generated by the upper Paleozoic coal bearing system laterally connected with the unconformity surface of the Majiagou Formation. Therefore, the natural gas continuously flowed into and charged the formation which manifested as the current mixed gas of oil type and coal derived gas.

5.2 Types of natural gas

There are two ways to generate organic thermogenic natural gas, and one is the primary cracking of kerogen and the other is cracking of oil or wet gas (Behar et al., 1922). Based on gas generation simulations under a gold tube system, a new discrimination plot of ln (C_1/C_2) *versus* ln (C_2/C_3) for gases of kerogen thermal cracking and oil thermal cracking at different thermal maturation stages was established and used widely with good application performance (Xie et al., 2016). According to this plot, the Ordovician natural gas was

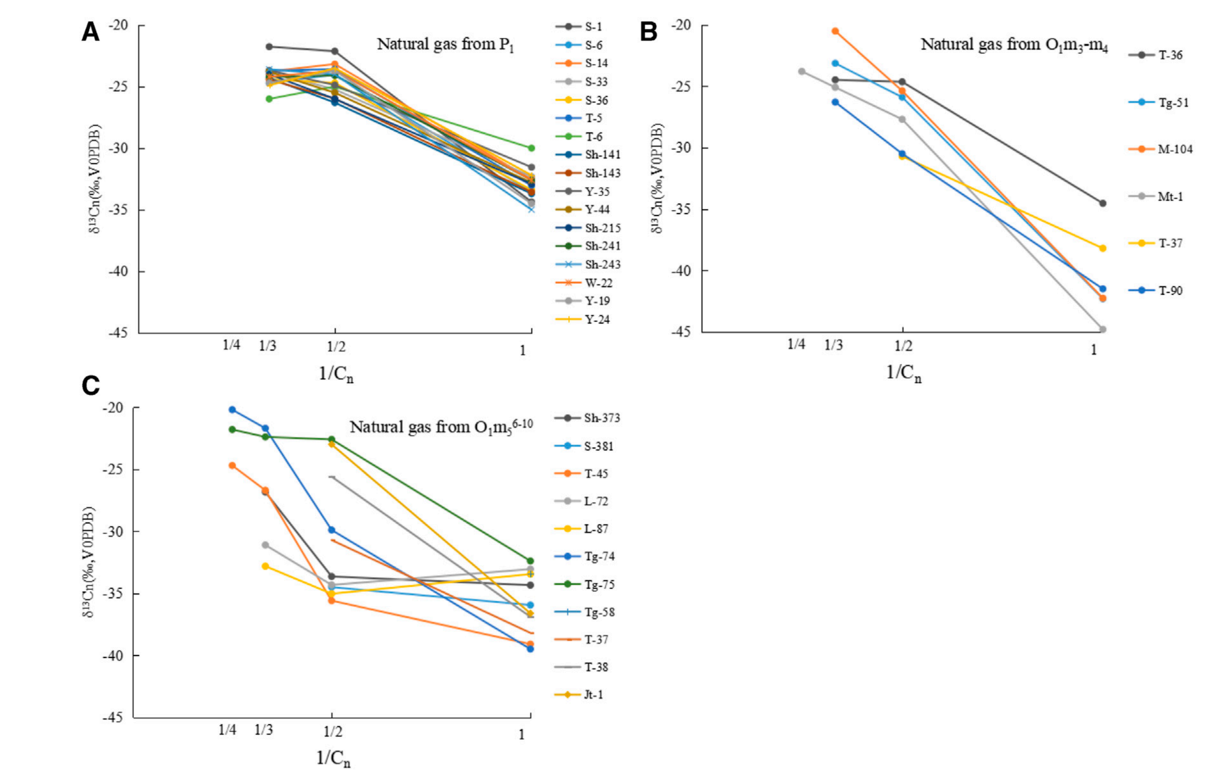

FIGURE 4
Relationship between carbon number 1/n and $\delta^{13}C_n$ of natural gas in the Ordos Basin **(A)** upper Paleozoic gas in the Ordos Basin, **(B)** O_1m_3 gas in the Ordos Basin, **(C)** $O_1m_5^{6-10}$ gas in the Ordos Basin.

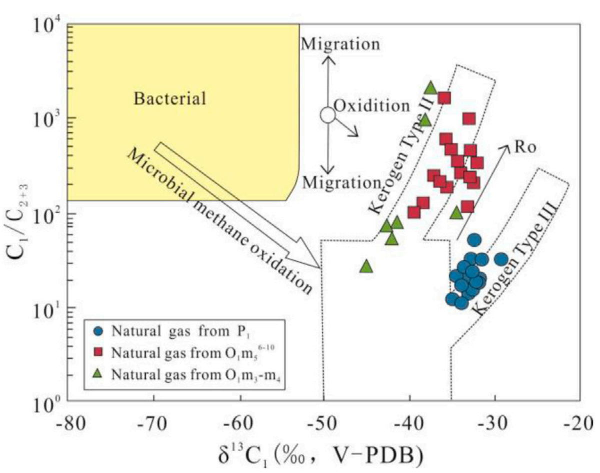

FIGURE 5
Relationship between C_1/C_{2+3} and $\delta^{13}C_1$ of natural gas in the Ordos Basin (Bernard et al., 1978, Modified)

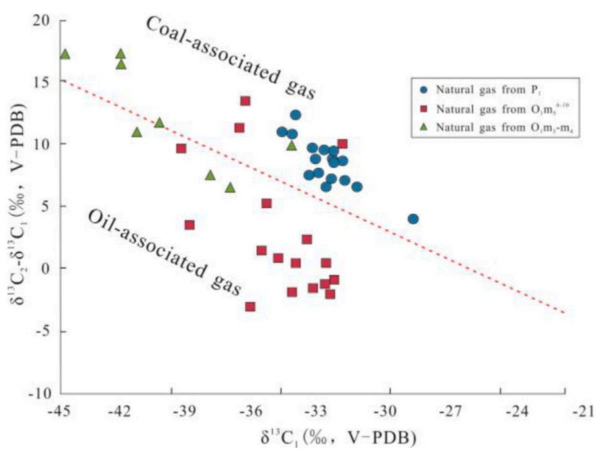

FIGURE 6
Relationship between ($\delta^{13}C_2$-$\delta^{13}C_1$) and $\delta^{13}C_1$ of natural gas in the Ordos Basin (Li et al., 2017)

mainly oil cracking gas with the maturity higher than 1.5% (Figure 7), while the upper Paleozoic natural gas was kerogen degradation gas with the maturity of 1.0%–1.5%. Previous studies showed that carbon isotope of CH_4 in organic thermogenic gas is mainly dependent on maturity (Dai and Qi, 1989). According to the regression equation ($\delta^{13}C_1 = 15.80\lg Ro-42.20$) between the maturity of natural gas and CH_4 carbon isotope ratio for oil-type gas (Dai, 1992), the maturity of the gas from O_1m_3 and O_1m_4 was between 1.6% and 2.1%, while that from $O_1m_5^{6-10}$ was 1.2%–2.1%. Furthermore, according to the regression equation ($\delta^{13}C_1 = 14.12\lg Ro-34.39$) between the maturity of natural gas and CH_4 carbon isotope for coal derived gas (Dai and Qi, 1989), the maturity of gas in the upper Paleozoic ranged from 1.1% to 1.4%, while the maturity of gas from $O_1m_5^{6-10}$ ranged from 0.8% to 1.2%,

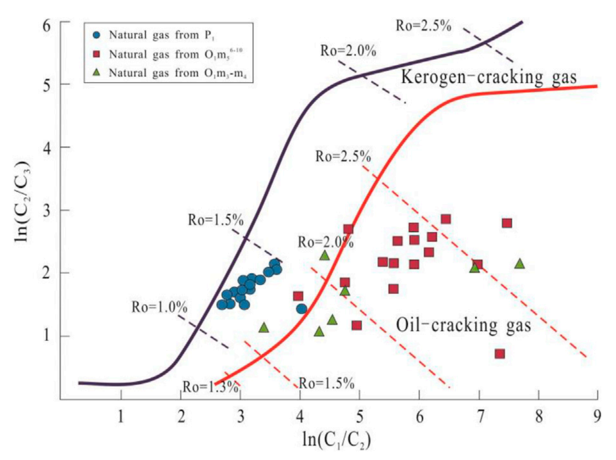

FIGURE 7
Plot of lnC_1/C_2 vs. lnC_2/C_3 to discriminate kerogen-cracking and oil-cracking gases with increasing Ro value.

which suggested that the natural gas from $O_1m_5^{6-10}$ was mixed by some coal derived gas from the upper Paleozoic coal.

5.3 Sources of H_2S

TSR occurs via chemical reactions involving hydrocarbons or organic matter at high temperatures, which consumes heavy hydrocarbons in natural gas and produces acidic gases such as H_2S and CO_2 (Hao et al., 2008; Tilley and Muehlenbachs, 2013). Numerous studies have been carried out on the H_2S of natural gas from the lower Paleozoic carbonate rock in the Sichuan and Tarim Basin, which show that TSR leads to a decrease in heavy hydrocarbon content of natural gas and increases in dryness and $\delta^{13}C_2$ value (Xie et al., 2021). There was no H_2S in upper Paleozoic natural gas of the Ordos Basin, which was primarily due to the fact that the upper Paleozoic natural gas reservoir is clastic rock. Some natural gas samples from Ordovician sub-salt of Majiagou Formation contained medium to high content of H_2S with high content of CO_2, such as Mt-1. Figure 8A shows that with the increasing H_2S content, $\delta^{13}C_2$ grows heavier and so does the gas dryness (all greater than 0.96), which mainly due to the TSR of carbonate rocks in the presence of heavy hydrocarbons. Furthermore, the range of $\delta^{13}C_1$ and C_1/C_{2+3} for upper Paleozoic natural gas were narrow, while those for the Majiagou Formation were large (Figure 8B), which also indicated that TSR occurred in the presence of heavy hydrocarbon gas in the Majiagou carbonate reservoir.

5.4 Accumulation of ordovician sub-salt natural gas

The genesis of Ordovician natural gas suggests that the Ordovician sub-salt reservoir has favorable hydrocarbon accumulation conditions owning to dual source hydrocarbon supply. Near the central paleo uplift, the Ordovician sub-salt reservoir directly contact with the upper Paleozoic coal, and the coal derived gas enters this high porous permeable dolomite reservoir through the fault and high porosity dolomite transport system, forming a source storage configuration of upper generation and lower reservoir. While on the east side of the central paleo-uplift, the Ordovician sub-salt reservoir is separated by thick overlying salt rock which plays the role of cap rock. Therefore, the Ordovician marine source rock is the main source rock and forms a typical self-generating and self-accumulating oil-type gas reservoir.

From the perspective of source reservoir cap configuration, the dolomite of O_1m_4 in the western part of the basin is thick, and gradually thins to the east. Although the western reservoir has large thickness, good physical properties and connectivity, it is directly contact with the upper Paleozoic coal and difficult to form effective traps due to the lack of overlying cap rocks and lateral sealing in the upward direction, which mainly plays the role of hydrocarbon supply window. While in the central and eastern part of the basin, the gas bearing property gradually becomes better with the development of overlying gypsum-salt cap rock. Therefore, the cap rock and preservation condition are very important for the Ordovician sub-salt gas accumulation (Figure 9). According to the trap forming conditions, O_1m_4 changes from dolomite facies to limestone facies from west to east (Ren et al., 2017). Under the paleotectonic background of high in the east and low in the west during the late Jurassic to early Cretaceous accumulation period, it is

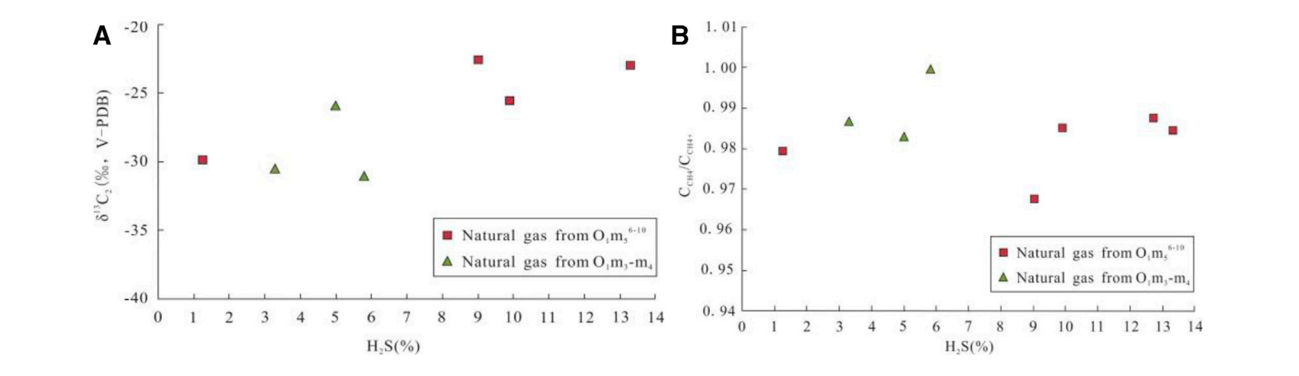

FIGURE 8
Relationship between $\delta^{13}C_2$ and H_2S **(A)**, C_{CH4}/C_{CH4+} and H_2S **(B)** of natural gas in the Ordos Basin.

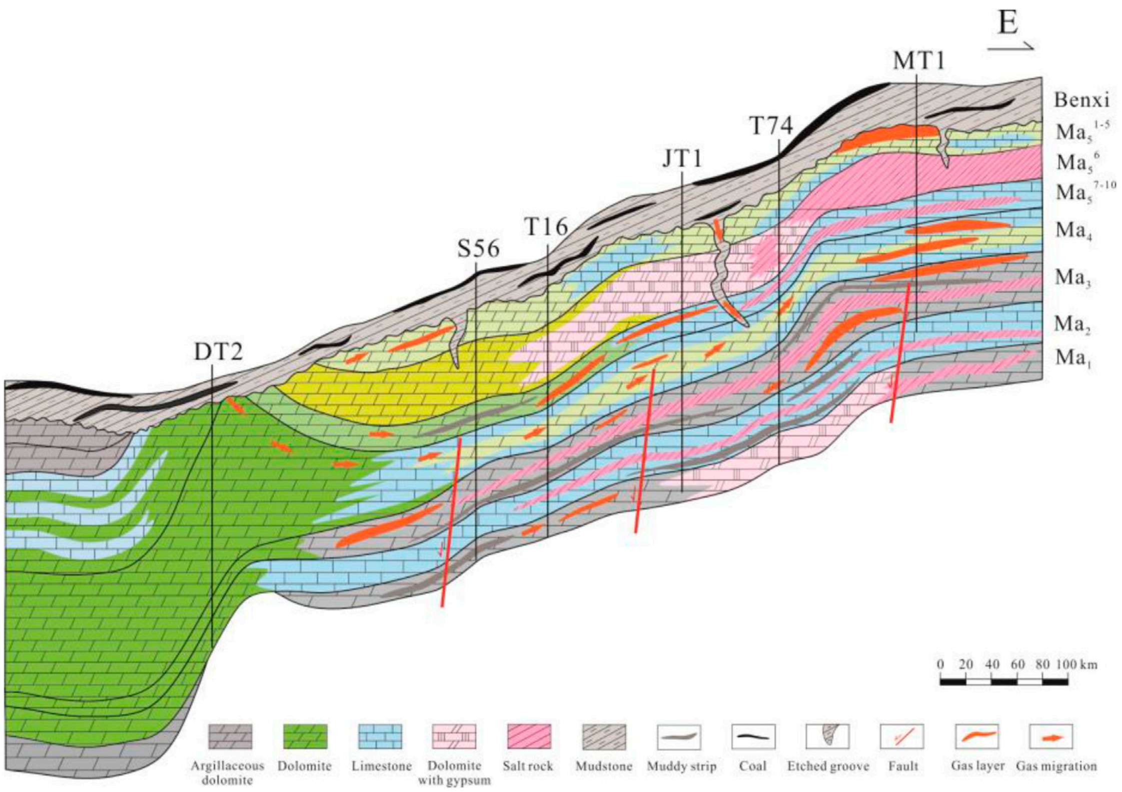

FIGURE 9
Gas accumulation pattern of Ordovician sub-salt reservoir of central eastern Ordos Basin (See Figure 1A for the location).

very conducive to the formation of dolomite lithologic traps and the formation of favorable areas for gas accumulation in large scale lithologic traps. Therefore, there is a good potential for natural gas exploration in Ordovician Sub-salt reservoir of central eastern Ordos Basin.

5.5 Implications for hydrocarbon exploration and development

The Ordovician sub-salt in Ordos Basin is a new exploration field. Through the analysis of the genetic types of natural gas, it is showed that the sub-salt natural gas is mainly derived from its own marine source rocks, which indicates that the sub-salt source rock has the basis of hydrocarbon accumulation. Besides, the sub-salt strata also have coal-derived gas generated from upper Paleozoic coal and forms the upper source and lower reservoir gas fields near the central paleo uplift. Owing to dual source hydrocarbon supply and thick layer of gypsum salt rock as good regional cap rock, the Ordovician sub-salt has good natural gas accumulation conditions and is the promising field of natural gas exploration and development in Ordos Basin.

Our results offer a reasonable explanation for the anomalous geochemical characteristics of the Ordovician sub-salt reservoirs in the Ordos Basin, supporting the view that the Ordovician sub-salt natural gas is mainly generated by lower Ordovician Marine source rocks with low organic matter. This study further makes clear that the Ordovician sub-salt natural gas is mainly oil-cracking gas with high maturity distributed in the central eastern Ordos Basin while the mixed gas near the central paleo uplift. Overall, the Ordovician sub-salt layers have good condition of gas accumulation owing to dual source hydrocarbon supply and the special sealing effect of evaporated gypsum rock.

Evaporated gypsum-salt rocks and oil and gas bearing properties in sedimentary basins are closely related. For example, the Paradox Basin and Green River Basin in the northwestern United States, Badenian evaporite basin of the Carpathian foredeep and Gulf of Mexico widely developed evaporites, which not only have good effective sealing effect, but also have good configuration relationship with source rocks and reservoirs in time and space and forms many large oil and gas fields (Jowettet al., 1993; Kasprzyk, 2003; Warren, 2010). The work we have done for the Ordos Basin will serve as a guide in the future when it comes to the exploration of natural gas in the carbonate gypsum-salt sedimentary system in these petroliferous basins, especially in the carbonate strata where the abundance of organic matter is low.

6 Conclusion

The natural gas of Ordovician sub-salt in the central eastern Ordos Basin was typically dry gas which is mainly high to over mature oil-cracking gas mixed with a small quantity of mature kerogen degradation gas. Non-hydrocarbon gases were predominately N_2 and CO_2, and a few samples contained H_2S which was generated from TSR.

The carbon isotope ratio of alkane gas in the Ordovician sub-salt mainly shows $\delta^{13}C_1 < \delta^{13}C_2 < \delta^{13}C_3 < \delta^{13}C_4$ (positive carbon isotope sequence), while some samples exhibit partial reversal ($\delta^{13}C_1 < \delta^{13}C_2 > \delta^{13}C_3$, and $\delta^{13}C_1 > \delta^{13}C_2 < \delta^{13}C_3$) which was mostly caused by mixing with coal derived gas sourced from upper Paleozoic and gas with different thermal maturities and TSR.

The natural gas of Ordovician sub-salt has good hydrocarbon accumulation conditions owning to dual source hydrocarbon supply and good regional gypsum cap rock. Oil-cracking gas is mainly distributed on the east side of the central paleo-uplift, while the coal-derived gas and mixed gas distributed near the central paleo uplift.

This study provides a reasonable explanation for the anomalous geochemical characteristics of the Ordovician sub-salt reservoirs in the Ordos Basin. It also offers that the deep Ordovician sub-salt layers have huge exploration potential for Ordos Basin natural gas exploration. Our work may serve as a reference for future investigations into natural gas in other basins' carbonate gypsum-salt sedimentary system.

Data availability statement

The raw data supporting the conclusion of this article will be made available by the authors, without undue reservation.

Author contributions

JS: Formal Analysis, Investigation, Software, Writing–original draft. YG: Methodology, Supervision, Writing–review and editing. JL: Conceptualization, Data curation, Funding acquisition, Methodology, Writing–review and editing. GD: Software, Visualization, Writing–original draft. XJ: Resources, Supervision, Writing–review and editing. GL: Writing–original draft. JH: Formal Analysis, Visualization, Writing–review and editing. CF: Conceptualization, Investigation, Writing–original draft. TZ: Writing–review and editing.

Funding

The author(s) declare financial support was received for the research, authorship, and/or publication of this article. The work was funded by the China Petroleum Science and Technology Project (Grant No. 2021DJ0601) and the Hubei Provincial Natural Science Foundation of China (Grant No. 2021CFB182).

Conflict of interest

Authors JS and JH were employed by PetroChina Research Institute of Petroleum Exploration and Development Northwest Branch. Authors JL and CF were employed by PetroChina Research Institute of Petroleum Exploration and Development. Authors GD, XJ and, GL were employed by Exploration and Development Institute of PetroChina Changqing Oilfield Company.

The remaining authors declare that the research was conducted in the absence of any commercial or financial relationships that could be construed as a potential conflict of interest.

Publisher's note

References

Bao, H. P., Wang, Q. P., Yan, W., Cai, Z. H., Zheng, J., Wei, L. B., et al. (2023). Sedimentary characteristics and gas accumulation potential of the Ordovician carbonate gypsum-salt rock interactive system in central-eastern Ordos Basin. *Earth Sci. Front.* 30 (1), 30–44. doi:10.13745/j.esf.sf.2022.8.25

Behar, F. S., Kressmann, S., Rudkiewicz, J. L., and Vandenbroucke, M. (1992). Experimental simulation in a confined system and kinetic modelling of kerogen and oil cracking. *Org. Geochem.* 19, 173–189. doi:10.1016/0146-6380(92)90035-v

Bernard, B. B., Brooks, J. M., and Sackett, W. M. (1978). Light hydrocarbons in recent Texas continental shelf and slope sediments. *J. Geophys. Res-Oceans* 83, 4053–4061. doi:10.1029/jc083ic08p04053

Boreham, C. J., and Edwards, D. S. (2008). Abundance and carbon isotopic composition of neo-pentane in Australian natural gases. *Org. Geochem.* 39, 550–566. doi:10.1016/j.orggeochem.2007.11.004

Burruss, R. C., and Laughrey, C. D. (2010). Carbon and hydrogen isotopic reversals in deep basin gas: evidence for limits to the stability of hydrocarbons. *Org. Geochem.* 41, 1285–1296. doi:10.1016/j.orggeochem.2010.09.008

Chung, H. M., Gormly, J. R., and Squires, R. M. (1988). Origin of gaseous hydrocarbons in subsurface environments: theoretical considerations of carbon isotope distribution. *Chem. Geol.* 71, 97–104. doi:10.1016/0009-2541(88)90108-8

Dai, J. X. (1992). Discrimination of all kinds of alkane gas. *Sci. China Ser. B* 2, 185–193.

Dai, J. X., Ni, Y. Y., Dong, D. Z., Qin, S. F., Zhu, G. Y., Huang, S. P., et al. (2021). 2021-2025 is a period of great development of China's natural gas industry: suggestions on the exploration and development of natural gas during the 14th Five-Year Plan in China. *Nat. Gas. Geosci.* 32 (1), 183–197. doi:10.1016/j.jnggs.2021.08.001

Dai, J. X., and Qi, H. F. (1989). Relationship of $\delta^{13}C$-Ro of coal-derived gas in China. *China Sci. B* 34, 690–692.

Dai, J. X., Xia, X. Y., Qin, S. F., and Zhao, J. Z. (2003). Causation of partly reversed orders of $\delta^{13}C$ in biogenic alkane gas in China. *Oil Gas. Geol.* 24 (1), 2–6. doi:10.3321/j.issn:0253-9985.2003.01.001

Dai, J. X., Yu, C., Huang, S. P., Gong, D. Y., Wu, W., Fang, C. C., et al. (2014). Geological and geochemical characteristics of large gas fields in China. *Petrol. explor. Dev.* 41 (1), 1–13. doi:10.1016/s1876-3804(14)60001-x

Du, J. H., Li, X. B., Bao, H. P., Xu, W. L., Wang, Y. T., Huang, J. P., et al. (2019). Geological conditions of natural gas accumulation and new exploration areas in the Mesoproterozoic to Lower Paleozoic of Ordos Basin, NW China. *Petrol. explor. Dev.* 46 (5), 866–882. doi:10.1016/s1876-3804(19)60246-6

Feng, Z. Q., Liu, D., Huang, S. P., Gong, D. Y., and Peng, W. L. (2016). Geochemical characteristics and genesis of natural gas in the Yan'an gas field, Ordos Basin, China. *China. Org. geochem.* 102, 67–76. doi:10.1016/j.orggeochem.2016.10.008

Fu, J. H., Dong, G. D., Zhou, X. P., Hui, X., Dan, W. D., Fan, L. Y., et al. (2021a). Research progress of petroleum geology and exploration technology in Ordos Basin. *China Pet. explor.* 26 (3), 19–40. doi:10.3969/j.issn.1672-7703.2021.03.003

Fu, J. H., Fan, L. Y., Liu, X. S., Hu, X. Y., Li, J. H., and Ji, H. K. (2019). New progresses, prospects and countermeasures of natural gas exploration in the Ordos Basin. *China Pet. explor.* 24 (4), 418–430. doi:10.3969/j.issn.1672-7703.2019.04.002

Fu, J. H., Wei, X. S., Ren, J. F., and Zhou, H. S. (2006). Gas exploration and developing prospect in Ordos Basin. *Acta. Petrol. Sin.* 27 (6), 1–13. doi:10.3321/j.issn:0253-2697.2006.06.001

Fu, S. T., Fu, J. H., Xi, S. L., and Huang, Z. L. (2021b). Geological characteristics of Ordovician marine shale gas in the Ordos Basin and its prospects. *China Pet. explor.* 26 (2), 33–44. doi:10.3969/j.issn.1672-7703.2021.02.004

Hao, F., Guo, T. L., Zhu, Y. M., Cai, X. Y., Zou, H. Y., and Li, P. P. (2008). Evidence for multiple stages of oil cracking and thermochemical sulfate reduction in the Puguang gas field, Sichuan Basin, China. *AAPG Bull.* 92, 611–637. doi:10.1306/01210807090

He, H. Q., Guo, X. J., Zhao, Z. Y., Xi, S. L., Wang, J. F., Song, W., et al. (2022). New understandings on gas accumulation and major exploration breakthroughs in subsalt ma 4 member of ordovician Majiagou Formation, Ordos Basin, NW China. *Petrol. explor. Dev.* 49 (3), 489–501. doi:10.1016/s1876-3804(22)60041-7

Jia, C. Z., Zhang, Y. F., and Zhao, X. (2014). Prospects of and challenges to natural gas industry development in China. *Nat. Gas. Ind.* 34 (2), 8–18. doi:10.3787/j.issn.1000-0976.2014.02.001

Jowett, E. C., Cathles, L. M., and Davis, B. W. (1993). Predicting depths of gypsum dehydration in evaporitic sedimentary. *AAPG Bull.* 77 (3), 403–405.

Kasprzyk, A. (2003). Sedimentological and diagenetic patterns of anhydrite deposits in the Badenian evaporite basin of the Carpathian foredeep, southern Poland. *Sediment. Geol.* 158 (3), 167–194. doi:10.1016/s0037-0738(02)00265-8

Kong, Q. F., Zhang, W. Z., Li, J. F., and Zan, C. L. (2019). Geochemical characteristics and genesis of Ordovician natural gas under gypsolyte in Ordos Basin. *Nat. Gas. Geosci.* 30 (3), 423–432. doi:10.11764/j.issn.1672-1926.2018.12.020

Li, J., Li, J., Li, Z. S., Zhang, C. L., Cui, H. Y., and Zhu, Z. L. (2018). Characteristics and genetic types of the lower paleozoic natural gas, Ordos Basin. *Mar. Petrol. Geol.* 89, 106–119. doi:10.1016/j.marpetgeo.2017.06.046

Li, J., She, Y. Q., Gao, Y., Yang, G. R., Li, M. P., and Yang, S. (2019). Onshore deep and ultra-deep natural gas exploration fields and potentials in China. *China Pet. explor.* 24 (4), 403–417. doi:10.3969/j.issn.1672-7703.2019.04.001

Li, L. G. (2021a). Development of natural gas industry in China: review and prospect. *Nat. Gas. Ind.* 41 (8), 1–11. doi:10.3787/j.issn.1000-0976.2021.08.001

Li, W., Tu, J. Q., Zhang, J., and Zhang, B. (2017). Accumulation and potential analysis of self-sourced natural gas in the ordovician Majiagou Formation of Ordos Basin, NW China. *Petrol. explor. Dev.* 44 (4), 552–562. doi:10.1016/s1876-3804(17)30064-2

Li, X. B., Wang, H. B., Huang, J. P., Zhang, C. L., Zhang, Y., Wang, Y. T., et al. (2021b). Characteristics of unconformity resulted from Huaiyuan Movement in Ordos Basin and its significance for oil and gas exploration. *Oil Gas. Geol.* 42 (5), 1043–1055. doi:10.11743/ogg20210503

Littke, R., Krooss, B. M., Idiz, E., and Frielingsdorf, J. (1995). Molecular nitrogen in natural gas accumulations: generation from sedimentary organic matter at high temperatures. *AAPG Bull.* 79 (3), 410–430. doi:10.1306/8d2b1548-171e-11d7-8645000102c1865d

Liu, C. Y., Wang, J. Q., Zhang, D. D., Zhao, H. G., Zhao, J. F., Huang, L., et al. (2021). Genesis of rich hydrocarbon resources and their occurrence and accumulation characteristics in the Ordos Basin. *Oil Gas. Geol.* 42 (5), 1011–1029. doi:10.11743/ogg20210501

Liu, D., Zhang, W. Z., Kong, Q. F., Feng, Z. Q., Fang, C. C., and Peng, W. L. (2016). Lower Paleozoic source rocks and natural gas origins in Ordos Basin, NW China. *Petrol. explor. Dev.* 43 (4), 591–601. doi:10.1016/s1876-3804(16)30069-6

Liu, Q. Y., Dai, J. X., Liu, W. H., Qin, S. F., and Zhang, D. W. (2007). Geochemical characteristics and genesis of nitrogen in natural gas from Tarim Basin. *Oil Gas. Geol.* 28 (1), 13–16. doi:10.3321/j.issn:0253-9985.2007.01.002

Niu, T., Hua, K., Xiao, D., Gao, X., Chen, J. P., and Cao, J. (2019). Tightness and sweet spot formation in moldic-pore-type dolomite reservoirs: the middle Ordovician Majiagou Formation in the eastern Ordos Basin,central China. *Petroleum* 5, 341–351. doi:10.1016/j.petlm.2019.03.004

Prinzhofer, A. A., and Huc, A. Y. (1995). Genetic and post-genetic molecular and isotopic fractionations in natural gases. *Chem. Geol.* 126 (3-4), 281–290. doi:10.1016/0009-2541(95)00123-9

Ren, J. F., Liu, X. S., Yu, J., Wei, L. B., and Wang, Q. P. (2021a). Characteristics of natural gas accumulation and exploration target of the Ordovician subsalt in the central and eastern Ordos Basin. *China Pet. explor.* 26 (6), 125–140. doi:10.3969/j.issn.1672-7703.2021.06.009

Ren, Z. L., Qi, K., Li, J. B., Huo, X. J., Cui, J. P., Yang, P., et al. (2021b). Thermodynamic evolution and hydrocarbon accumulation in the Ordos Basin. *Oil Gas. Geol.* 42 (5), 1030–1042. doi:10.11743/ogg20210502

Ren, Z. L., Yu, Q., Cui, J. P., Qi, K., Chen, Z. J., Cao, Z. P., et al. (2017). Thermal history and its controls on oil and gas of the Ordos Basin. *Earth Sci. Front.* 24 (3), 137–148. doi:10.13745/j.esf.2017.03.012

Rooney, M. A., Claypool, G. E., Chung, H. M., and Moses, H. (1995). Modeling thermogenic gas generation using carbon isotope ratios of natural gas hydrocarbons. *Chem. Geol.* 126, 219–232. doi:10.1016/0009-2541(95)00119-0

Shao, D. P., Bao, H. P., Wei, L. B., Cai, Z. H., and Wu, C. Y. (2019). Tectonic palaeogeography evolution and sedimentary filling characteristics of the Ordovician in the Ordos area. *J. Palaeog.* 21 (4), 537–556. doi:10.7605/gdlxb.2019.04.035

Shen, A. Q., Liu, Y. K., Wang, X., Cai, B., He, C. M., and Liang, S. (2019). The geological characteristics and exploration of continental tight oil: an investigation in China. *J. Pet. Explor. Prod. Te.* 9, 1651–1658. doi:10.1007/s13202-018-0606-5

Tilley, B., and Muehlenbachs, K. (2013). Isotope reversals and universal stages and trends of gas maturation in sealed, self-contained petroleum systems. *Chem. Geol.* 339, 194–204. doi:10.1016/j.chemgeo.2012.08.002

Warren, J. K. (2010). Evaporites through time: tectonic, climatic and eustatic controls in marine and nonmarine deposits. *Earth-Sci. Rev.* 98 (3/4), 217–268. doi:10.1016/j.earscirev.2009.11.004

Whiticar, M. J. (1999). Carbon and hydrogen isotope systematics of bacterial formation and oxidation of methane. *Chem. Geol.* 161, 291–314. doi:10.1016/s0009-2541(99)00092-3

Wu, D. X., Yu, J., Zhou, J. G., Wu, X. N., Yu, Z., Ding, Z. C., et al. (2021). Sedimentary characteristics and reservoir controlling effect of the member 4 of ordovician Majiagou Formation in Ordos Basin. *J. Palaeog.* 23 (6), 1140–1157. doi:10.7605/gdlxb.2021.06.073

Xie, Z. Y., Li, J., Yang, C. L., Tian, X. W., Zhang, L., Li, J., et al. (2021). Geochemical characteristics of Sinian-Cambrian natural gas in central Sichuan paleo-uplift and exploration potential of Taihe gas area. *Nat. Gas. Ind.* 41 (7), 1–14. doi:10.3787/j.issn.1000-0976.2021.07.001

Xie, Z. Y., Li, Z. S., Wei, G. Q., Li, J., Wang, D. L., Wang, Z. H., et al. (2016). Experimental research on the potential of sapropelic kerogen degradation gas and discrimination of oil cracking gas. *Nat. Gas. Geosci.* 27 (6), 1057–1066. doi:10.11764/j.issn.1672-1926.2016.06.1057

Yang, H., Liu, X. S., and Zhang, D. F. (2013). Main controlling factors of gas pooling in Ordovician marine carbonate reservoirs in the Ordos Basin and advances in gas exploration. *Nat. Gas. Ind.* 33 (5), 1–12. doi:10.3787/j.issn.1000-0976.2013.05.001

Zhao, W. Z., Wang, Z. C., Jiang, H., Fu, X. D., Xie, W. R., Xu, A. N., et al. (2020). Exploration status of the deep Sinian strata in the Sichuan Basin: formation conditions of old giant carbonate oil and gas fields. *Nat. Gas. Ind.* 40 (2), 1–10. doi:10.3787/j.issn.1000-0976.2020.02.001

Zhu, G. Y., Zhang, S. C., Li, J., and Jin, Q. (2004). Formation and distribution of hydrogen sulfide bearing gas in China. *Petrol. explor. Dev.* 31 (3), 18–21. doi:10.3321/j.issn:1000-0747.2004.03.005

Zou, C. N., Xie, Z. Y., Li, J., Zhang, L., Yang, C. L., Cui, H. Y., et al. (2023). Differences and main controlling factors of large-scale gas accumulations in typical giant carbonate gas fields: a case study on Anyue gas field in the Sichuan Basin and Jingbian gas field in the Ordos Basin. *Oil Gas. Geol.* 44 (1), 1–15. doi:10.11743/ogg20230101